Supplement of Atmos. Chem. Phys., 24, 6095–6103, 2024
https://doi.org/10.5194/acp-24-6095-2024-supplement

Atmospheric Chemistry and Physics
Open Access
EGU

Supplement of

The impact of gaseous degradation on the gas–particle partitioning of methylated polycyclic aromatic hydrocarbons

Fu-Jie Zhu et al.

Correspondence to: Wan-Li Ma (mawanli002@163.com)

Contents

Text S1. The derivation of the log K_P' for LMW SVOCs based on the new steady-state G–P partitioning model

The gas–particle (G–P) partitioning quotient (K_P') can be calculated as follows:

$$K_P' = (C_P/C_G)/TSP \quad \text{(S1)}$$

where, C_P (ng/m^3 air) and C_G (ng/m^3) are the concentrations of SVOCs in particle phase and gas phase, respectively, and *TSP* is the concentrations of total suspended particles (μg/m^3).

C_P can be transferred to C'_P (ng/m^3 particle) based the following equation:

$$C_P = C'_P \times TSP/10^9\rho_P \quad \text{(S2)}$$

where, C'_P (ng/m^3 particle) is the concentrations in particle phase with different units, and ρ_P is the density of particles (kg/m^3).

Then, the Eq. (S1) can be expressed in different form:

$$K_P' = (C'_P/C_G)/10^9\rho_P \quad \text{(S3)}$$

The ratio of C'_P to C_G can be calculated using the method from the multimedia fugacity model:

$$C'_P/C_G = f_P Z_P/f_G Z_G \quad \text{(S4)}$$

where, f_P and f_G are the fugacity for particle phase and gas phase, respectively, Z_P and Z_G are the fugacity capacity for particle phase and gas phase, respectively.

Z_P/Z_G equal to K_{PG} at equilibrium state, which can be calculated by the following equation (Li et al., 2015):

$$K_{PG} = Z_P/Z_G = 10^9\rho_P K_{P-HB} \quad \text{(S5)}$$

where, $K_{P\text{-}HB}$ is the G–P partitioning coefficient calculated from the H-B model (the equilibrium-state model) (Harner and Bidleman, 1998).

Summarizing the equations above, log K_P can be expressed as following equation:

$$\log K_P' = \log K_{P-HB} + \log(f_P/f_G) \quad \text{(S6)}$$

According to the Eq. (5), K_P' will upward deviate from $K_{P\text{-}HB}$ (or the equilibrium state) when $f_P > f_G$. Based on our previous study (Zhu et al., 2023), the fugacity ratio of

the particle phase to the gas phase can be expressed as Eq. (S7), when the steady state is reached between gas phase and particle phase:

$$\frac{f_P}{f_G} = \frac{D_{GP}+\phi_0 D_{GR}}{D_{GP}+(1-\phi_0)(D_{PD}+D_{PW})} \quad (S7)$$

where, ϕ_0 is the particulate proportion of SVOCs in emission; D_{GP} is the intermedia D value between gas phase and particle phase; D_{GR} is the D value for the degradation of gas-phase SVOCs; D_{PD} and D_{PW} are the D values of the dry and wet depositions of particle-phase SVOCs, respectively.

For the LMW SVOCs, the dry and wet deposition fluxes of particle phase (F_{PD} + F_{PW}) (**Fig. S5**) can be ignored (Li et al., 2015; Zhu et al., 2023), then the Eq. (S7) can be expressed as follows:

$$\frac{f_P}{f_G} = 1 + \frac{\phi_0 D_{GR}}{D_{GP}} \quad (S8)$$

Based on the above equation, when $\phi_0 D_{GR}$ cannot be ignored compared with D_{GP}, f_P will be higher than f_G, and the K_P' values will deviate upward from equilibrium state. In other words, when $\phi_0 F_{GR}$ ($F_{GR} = f_G D_{GR}$, the degradation flux of gas phase) cannot be ignored compared with F_{GP} ($F_{GP} = f_G D_{GP}$, the flux from gas phase to particle phase), the K_P' values will deviate upward from equilibrium state. Therefore, it can be concluded that the deviation was affected by both the gaseous degradation and the particulate proportion of SVOCs in emission.

References:

Harner, T. and Bidleman, T. F.: Octanol-air partition coefficient for describing particle/gas partitioning of aromatic compounds in urban air, Environmental Science & Technology, 32, 1494-1502, https://doi.org/10.1021/es970890r, 1998.

Li, Y. F., Ma, W. L., and Yang, M.: Prediction of gas/particle partitioning of polybrominated diphenyl ethers (PBDEs) in global air: A theoretical study, Atmospheric Chemistry and Physics, 15, 1669-1681, https://doi.org/10.5194/acp-15-1669-2015, 2015.

Zhu, F. J., Hu, P. T., and Ma, W. L.: A new steady-state gas–particle partitioning model of polycyclic aromatic hydrocarbons: Implication for the influence of the particulate proportion in emissions, Atmospheric Chemistry and Physics, 23, 8583-8590, https://doi.org/10.5194/acp-23-8583-2023, 2023.

Table S1. Information of 49 Me-PAHs

Compounds	Abbreviations	Categories	Rings	Quantitative ions	Qualitative ions	Retention time (min)	IDLs[a] (ng)	DR[b]
2-Methylnaphthalene	2-MeNap	Me	2	142	141	6.858	0.0384	84%
1-Methylnaphthalene	1-MeNap	Me	2	142	141	6.991	0.0505	85%
2,6&2,7-Dimethylnaphthalene	2,6&2,7-DMeNap	Me	2	156	141	7.710	0.0154	46%
1,3-Dimethylnaphthalene	1,3-DMeNap	Me	2	156	141	7.844	0.0904	70%
1,6-Dimethylnaphthalene	1,6-DMeNap	Me	2	156	141	7.886	0.0857	73%
1,4&1,5-Dimethylnaphthalene	1,4&1,5-DMeNap	Me	2	156	141	8.086	0.0467	74%
1,2-Dimethylnaphthalene	1,2-DMeNap	Me	2	156	141	8.220	0.138	68%
1,8-Dimethylnaphthalene	1,8-DMeNap	Me	2	156	141	8.462	0.126	-
2-Methylphenanthrene	2-MePhe	Me	3	192	191	17.476	0.310	96%
2-Methylanthracene	2-MeAnt	Me	3	192	191	17.648	0.240	88%
1-Methylanthracene	1-MeAnt	Me	3	192	191	17.812	0.207	-
1-Methylphenanthrene	1-MePhe	Me	3	192	191	17.855	0.239	98%
9-Methylanthracene	9-MeAnt	Me	3	192	191	18.321	0.432	56%
3,6-Dimethylphenanthrene	3,6-DMePhe	Me	3	206	191	18.847	0.134	-
2,3-Dimethylanthracene	2,3-DMeAnt	Me	3	206	191	19.606	0.201	-
9-Methyl-9-phenylfluorene	9-Me-9-PFlu	Me	4	241	256	20.015	0.0335	-
9,10-Dimethylanthracene	9,10-DMeAnt	Me	3	206	191	20.155	0.245	-
2-Methylfluoranthene	2-MeFluo	Me	4	216	215	20.646	0.0636	97%
1-Methylpyrene	1-MePyr	Me	4	216	215	21.453	0.0620	97%
1-Methylbenzo[c]phenanthrene	1-MeBcP	Me	4	242	241	22.584	0.0570	92%
2-Methylbenzo[c]phenanthrene	2-MeBcP	Me	4	242	241	23.230	0.0275	84%

continued Table S1

Compounds	Abbreviations	Categories	Rings	Quantitative ions	Qualitative ions	Retention time (min)	IDLs[a] (ng)	DR[b]
3-Methylbenzo[c]phenanthrene	3-MeBcP	Me	4	242	241	23.623	0.0700	84%
5-Methylbenzo[c]phenanthrene	5-MeBcP	Me	4	242	241	23.800	0.0641	-
4-Methylbenzo[c]phenanthrene	4-MeBcP	Me	4	242	241	23.846	0.0673	-
1&2-Methylbenz[a]anthracene	1&2-MeBaA	Me	4	242	241	24.138	0.0367	74%
7&9-Methylbenz[a]anthracene	7&9-MeBaA	Me	4	242	241	24.254	0.0331	70%
6&4-Methylbenz[a]anthracene	6&4-MeBaA	Me	4	242	241	24.308	0.0313	62%
1,12-Dimethylbenzo[c]phenanthrene	1,12-DMeBcP	Me	4	256		24.469	0.0607	-
5&6&4-Methylchrysene & 3&5-Methylbenz[a]anthracene	5&6&4-MeChr&3&5-MeBaA	Me	4	242	241	24.500	0.0214	98%
10-Methylbenz[a]anthracene	10-MeBaA	Me	4	242	241	24.893	0.103	-
5,8-Dimethylbenzo[c]phenanthrene	5,8-DMeBcP	Me	4	256	239	25.270	0.0933	-
6,8-Dimethylbenz[a]anthracene	6,8-DMeBaA	Me	4	256	239	25.462	0.0908	-
3,9-Dimethylbenz[a]anthracene	3,9-DMeBaA	Me	4	256	239	25.578	0.108	50%
7,12-Dimethylbenz[a]anthracene	7,12-DMeBaA	Me	4	256	239	26.457	0.190	-
3-Methylcholanthrene	3-Me-Cho	Me	5	268	253	29.440	0.951	-
9-Methylbenzo[a]pyrene	9-MeBaP	Me	5	266	265	29.728	0.595	-
8-Methylbenzo[a]pyrene	8-MeBaP	Me	5	266	265	29.929	0.271	-
7&10-Methylbenzo[a]pyrene	7&10-MeBaP	Me	5	266	265	30.252	0.590	-
7,10-Dimethylbenzo[a]pyrene	7,10-DMeBaP	Me	5	280	131	33.153	0.505	-

Note: Underlined compounds represent that the instrumental method cannot achieve chromatographic separation for these compounds with same quantitative and qualitative ions.

a, represents instrument detection limits.

b, represents detection rate of all samples (include gaseous and particulate samples).

“-” represents the detection rate was below 30%.

Table S2. Values and the calculation parameters for *A* and *B* of several Me-PAHs

Compounds	E[a]	S[a]	A[a]	B[a]	V[a]	L[a]	log K_{OA} (25°C)[b]	ΔH_{OA} (kJ/mol)[b]	*A*[c]	*B*[c]
2-MeNap	1.3	0.81	0	0.25	1.2263	5.617	5.51	56.43	−4.38	2948
1-MeNap	1.34	0.94	0	0.22	1.2263	5.802	5.73	57.16	−4.28	2986
2,6-DMeNap	1.35	0.82	0	0.25	1.3672	6.146	6.01	61.26	−4.72	3200
2,7-DMeNap	1.35	0.82	0	0.25	1.3672	6.147	6.01	61.27	−4.72	3201
1,3-DMeNap	1.39	0.92	0	0.2	1.3672	6.236	6.1	61.07	−4.60	3190
1,6-DMeNap	1.37	0.94	0	0.21	1.3672	6.347	6.23	62.11	−4.65	3244
1,4-DMeNap	1.4	0.91	0	0.2	1.3672	6.339	6.19	62.12	−4.69	3245
1,5-DMeNap	1.4	1.05	0	0.18	1.3672	6.545	6.45	63.08	−4.60	3295
1,2-DMeNap	1.43	0.97	0	0.25	1.3672	6.473	6.38	63.51	−4.75	3318
1,8-DMeNap	1.4	1.01	0	0.21	1.3672	6.653	6.55	64.64	−4.78	3377
2-MePhe	2.06	1.25	0	0.29	1.5953	8.307	8.16	79.55	−5.78	4155
2-MeAnt	2.29	1.3	0	0.31	1.5953	8.184	8.04	78.25	−5.67	4088
1-MeAnt	2.29	1.3	0	0.3	1.5953	8.332	8.17	79.59	−5.77	4158
1-MePhe	2.06	1.25	0	0.29	1.5953	8.408	8.26	80.53	−5.85	4207
9-MeAnt	2.25	1.27	0	0.3	1.5953	8.438	8.27	80.79	−5.88	4220
3,6-DMePhe	2.05	1.29	0	0.29	1.7362	8.7	8.56	82.89	−5.96	4330
9,10-DMeAnt	2.25	1.25	0	0.28	1.7362	9.283	9.04	88.67	−6.50	4632
1-MePyr	2.81	1.7	0	0.26	1.7255	9.541	9.4	88.28	−6.07	4611
1-MeBaA	2.99	1.7	0	0.35	1.9643	10.763	10.58	100.54	−7.03	5252
7-MeBaA	2.99	1.7	0	0.35	1.9643	11.096	10.89	103.76	−7.29	5420
4-MeBaA	2.99	1.7	0	0.35	1.9643	10.909	10.72	101.95	−7.14	5326
5-MeChr	3.03	1.73	0	0.36	1.9643	10.905	10.73	101.82	−7.11	5319

continued Table S2

Compounds	E[a]	S[a]	A[a]	B[a]	V[a]	L[a]	log K_{OA} (25°C)[b]	ΔH_{OA} (kJ/mol)[b]	A[c]	B[c]
6-MeChr	3.03	1.73	0	0.36	1.9643	10.934	10.76	102.1	−7.13	5333
4-MeChr	3.03	1.73	0	0.36	1.9643	10.937	10.76	102.13	−7.13	5335
7,12-DMeBaA	2.99	1.65	0	0.35	2.1052	11.753	11.48	110.19	−7.83	5756
3-MeCho	3.26	1.57	0	0.51	2.1375	12.482	12.19	119.14	−8.68	6223

Note:

a, Ulrich, N., Endo, S., Brown, T.N., Watanabe, N., Bronner, G., Abraham, M.H., Goss, K.-U., UFZ-LSER database v 3.2.1 [Internet], Leipzig, Germany, Helmholtz Centre for Environmental Research-UFZ. 2017 [accessed on 09.08.2022]. Available from http://www.ufz.de/lserd.

b, log K_{OA} (25°C) and ΔH_{OA} (kJ/mol) were calculated using the parameters in **Table S1 and S2.**

c, B is calculated by the equation: $B = \Delta H_{OA} / (\ln(10) * 8.314)$, A is calculated by the equation: $A = \log K_{OA}$ (25°C) − B / 298.15.

Table S3. Calculation parameters for log K_{OA} (25°C) and ΔH_{OA} (kJ/mol)

Parameters	e	s	a	b	v	l	constant	Equations	References
log K_{OA} (25°C)	−0.21	0.56	3.51	0.75		0.94	−0.15	Parameter = l * L + s * S + a * A + b * B + e * E + constant	[1]
ΔH_{OA} (kJ/mol)		−6.04	53.66	9.19	−1.57	9.66	6.67	Parameter = l * L + s * S + a * A + b * B + v * V + constant	[2]

References:

[1] Abraham, M. H., Acree, W. E., Jr., Leo, A. J., Hoekman, D., and Cavanaugh, J. E.: Water-solvent partition coefficients and Δlog *P* values as predictors for blood-brain distribution; application of the akaike information criterion, Journal of Pharmaceutical Sciences, 99, 2492-2501, https://doi.org/10.1002/jps.22010, 2010.

[2] Mintz, C., Burton, K., Ladlie, T., Clark, M., Acree, W. E., Jr., and Abraham, M. H.: Enthalpy of solvation correlations for gaseous solutes dissolved in dibutyl ether and ethyl acetate, Thermochimica Acta, 470, 67-76, https://doi.org/10.1016/j.tca.2008.02.001, 2008.

Table S4. The geometric mean values of the N/D ratios for different phases Me-PAHs in different seasons

	Total Phase			Particle Phase			Gas Phase		
	All season	Heating season	Non-heating season	All season	Heating season	Non-heating season	All season	Heating season	Non-heating season
2-MeNap	**2.67**	**2.14**	**3.30**	0.842	**0.561**	2.23	**2.73**	**2.21**	**3.33**
1-MeNap	**3.16**	**2.22**	4.41	0.819	**0.493**	2.47	**3.25**	**2.30**	**4.51**
2,6&2,7-DMeNap	**2.19**	**2.02**	**7.30**	0.347	0.347	-	**2.37**	**2.19**	7.30
1,3-DMeNap	**2.97**	**2.01**	**4.27**	0.588	0.499	3.03	**3.03**	**2.11**	**4.27**
1,6-DMeNap	**2.76**	**1.93**	**3.85**	0.604	0.528	1.18	**2.83**	**2.03**	**3.87**
1,4&1,5-DMeNap	**2.67**	**1.88**	**3.72**	0.501	**0.429**	3.28	**2.73**	**1.96**	**3.72**
1,2-DMeNap	**2.45**	1.75	**3.35**	0.557	0.557	-	**2.49**	**1.82**	**3.35**
2-MePhe	1.11	1.12	1.10	1.09	0.984	1.24	1.11	1.14	1.09
2-MeAnt	1.20	1.32	1.11	1.68	1.34	**2.94**	1.04	1.05	1.03
1-MePhe	1.15	1.12	1.18	1.08	0.975	1.22	1.15	1.14	1.17
9-MeAnt	**2.07**	2.49	1.38	2.04	2.04	-	**1.89**	2.78	1.28
2-MeFluo	1.36	1.23	1.50	1.61	1.24	**2.05**	1.05	0.68	1.46
1-MePyr	**1.65**	1.39	**1.95**	**1.97**	1.40	**2.71**	**1.31**	0.81	**1.89**
1-MeBcP	1.93	1.25	**2.88**	1.83	1.30	**2.63**	**1.86**	1.01	**2.79**
2-MeBcP	1.73	1.26	**2.34**	**1.90**	1.27	**2.78**	1.56	1.12	1.72
3-MeBcP	1.61	1.27	**2.01**	1.67	1.26	**2.24**	1.45	1.15	1.54
1&2-MeBaA	**2.04**	1.57	**2.61**	**2.08**	1.56	**2.72**	1.79	0.87	2.70
7&9-MeBaA	1.69	1.35	2.11	1.61	1.34	**1.99**	1.22	1.48	1.15
6&4-MeBaA	**1.85**	1.44	**2.33**	**1.84**	1.44	**2.31**	1.22	-	1.22

continued Table S4

	Total Phase			Particle Phase			Gas Phase		
	All season	Heating season	Non-heating season	All season	Heating season	Non-heating season	All season	Heating season	Non-heating season
5&6&4-MeChr&3&5-MeBaA	**1.90**	1.46	**2.42**	**2.01**	1.46	**2.77**	1.31	1.17	1.46
3,9-DMeBaA	**1.86**	1.72	**2.01**	**1.86**	1.72	**2.01**	-	-	-
Number of significances	13	6	14	6	3	11	10	7	8

Note: The bold numbers represent the mean concentrations of Me-PAHs in nighttime were significant different with those in daytime ($p < 0.05$).

Table S5. Gaseous degradation rate (h^{-1}) (hydroxyl radicals reaction) of Me-Naps and U-PAHs under different temperatures

PAHs	k_{deg_25}	k_{deg_-50}	k_{deg_50}
2-MeNap	0.305	0.0787	0.417
1-MeNap	0.305	0.0787	0.417
2,6&2,7-DMeNap	0.375	0.0966	0.512
1,3-DMeNap	0.375	0.0966	0.512
1,6-DMeNap	0.375	0.0966	0.512
1,4&1,5-DMeNap	0.375	0.0966	0.512
1,2-DMeNap	0.375	0.0966	0.512
acenaphthylene	0.408	0.118	0.557
acenaphthene	0.361	0.105	0.493
fluorene	0.0478	0.0139	0.0653

Note: The gaseous degradation rate of PAHs can be calculated using the half-lives of PAHs: $k_{degi} = \ln(2)/t_{1/2}$, and the half-lives of PAHs were calculated from EPI suite.

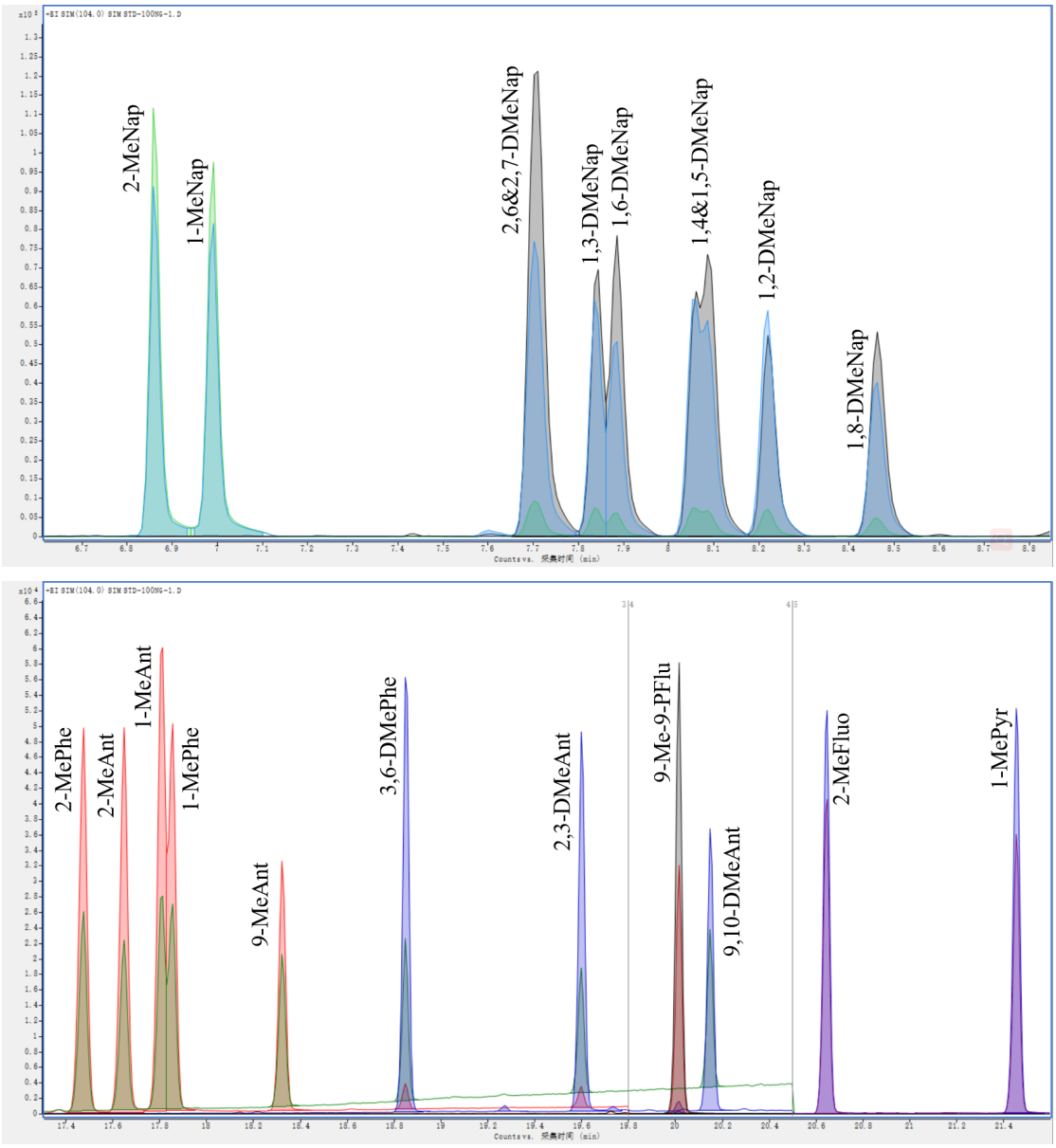
2-MeNap
1-MeNap
2,6&2,7-DMeNap
1,3-DMeNap
1,6-DMeNap
1,4&1,5-DMeNap
1,2-DMeNap
1,8-DMeNap
2-MePhe
2-MeAnt
1-MeAnt
1-MePhe
9-MeAnt
3,6-DMePhe
2,3-DMeAnt
9-Me-9-PFlu
9,10-DMeAnt
2-MeFluo
1-MePyr

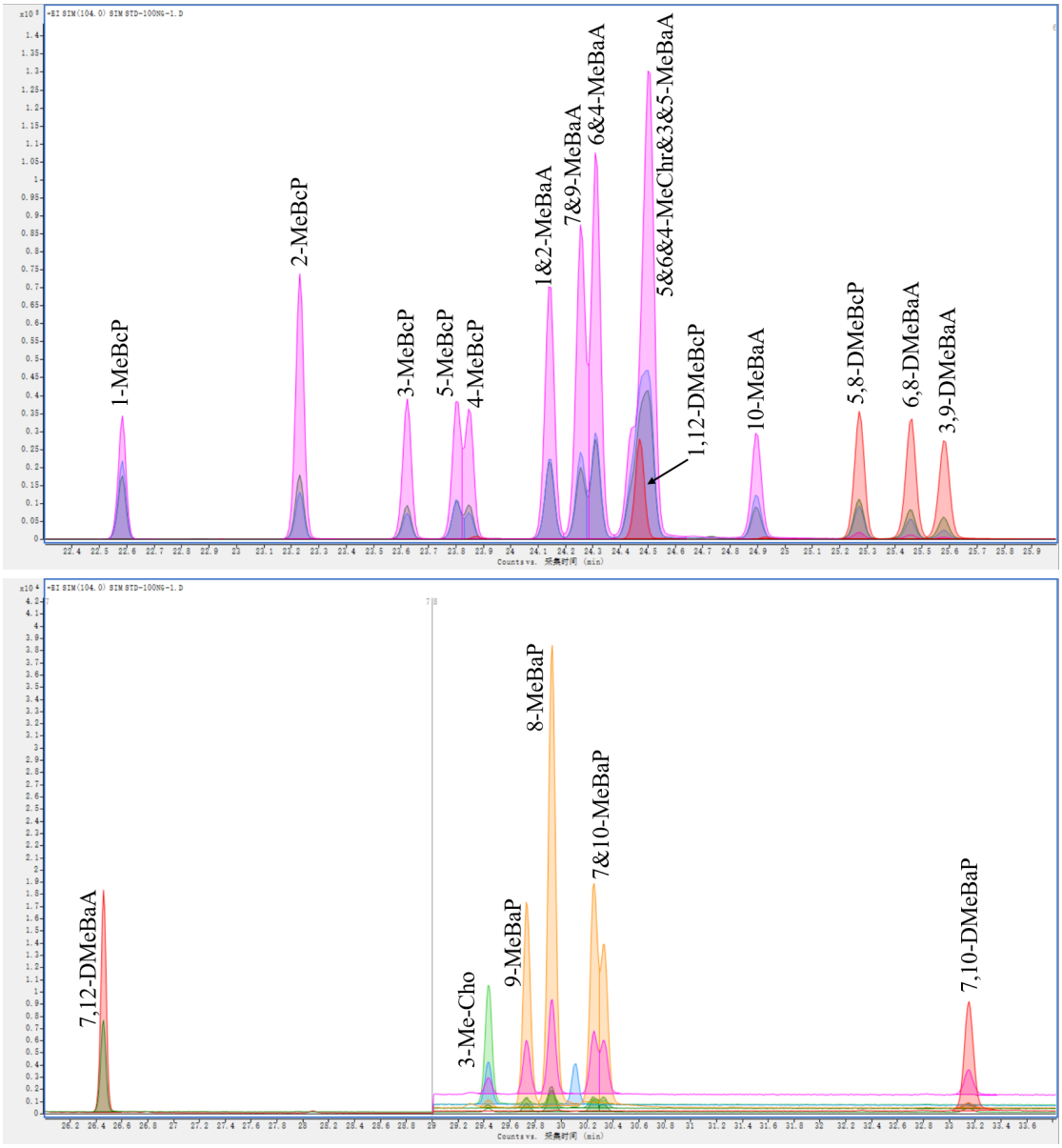

Fig. S1. Chromatographic separation of 49 Me-PAHs in standard solutions (100 ng/mL)

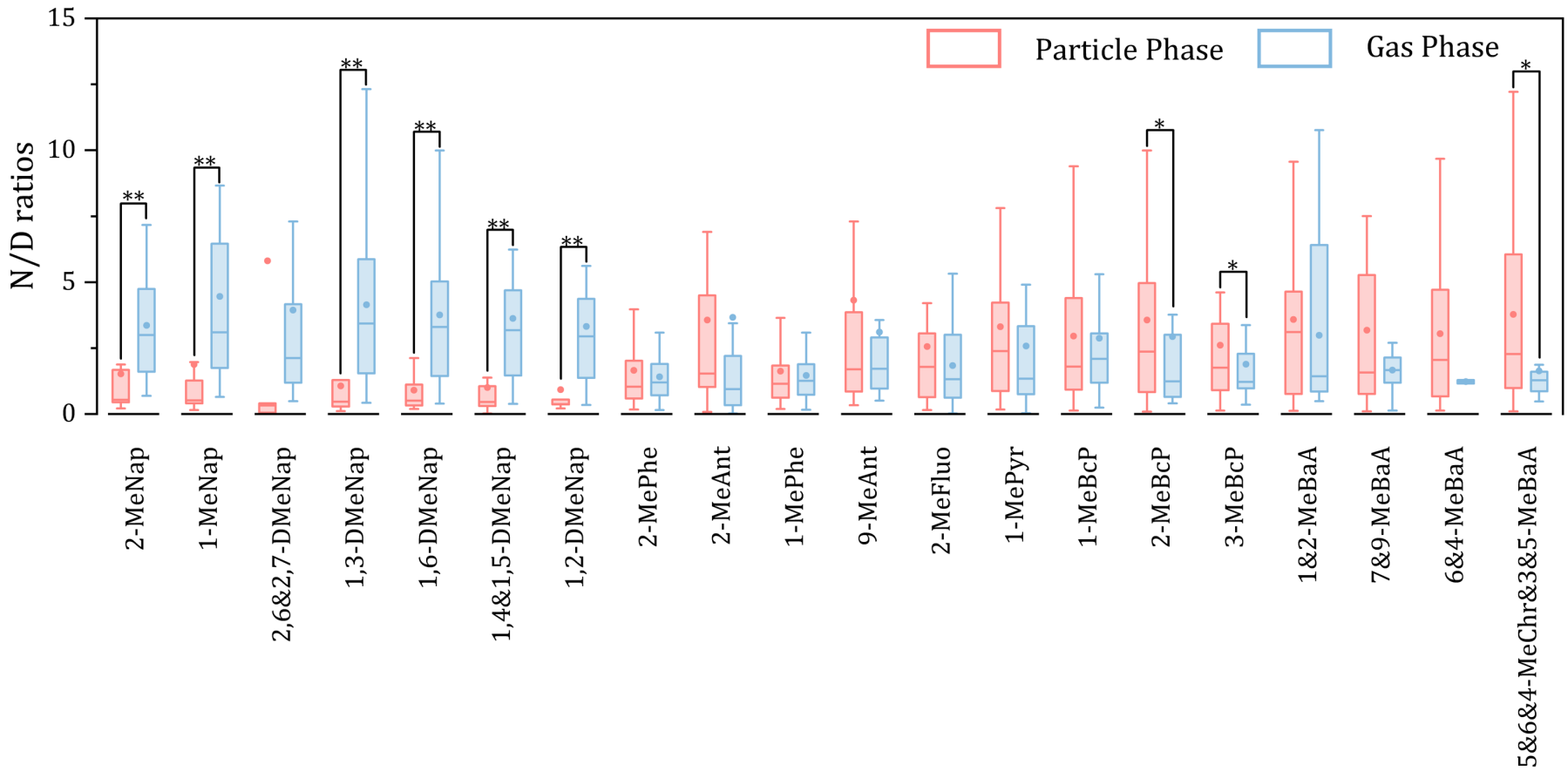

Fig. S2. Comparison of the values of N/D ratios for individual Me-PAHs between particle phase and gas phase

(Note: * and ** represent that the differences are significant at 0.05 and 0.01 level.)

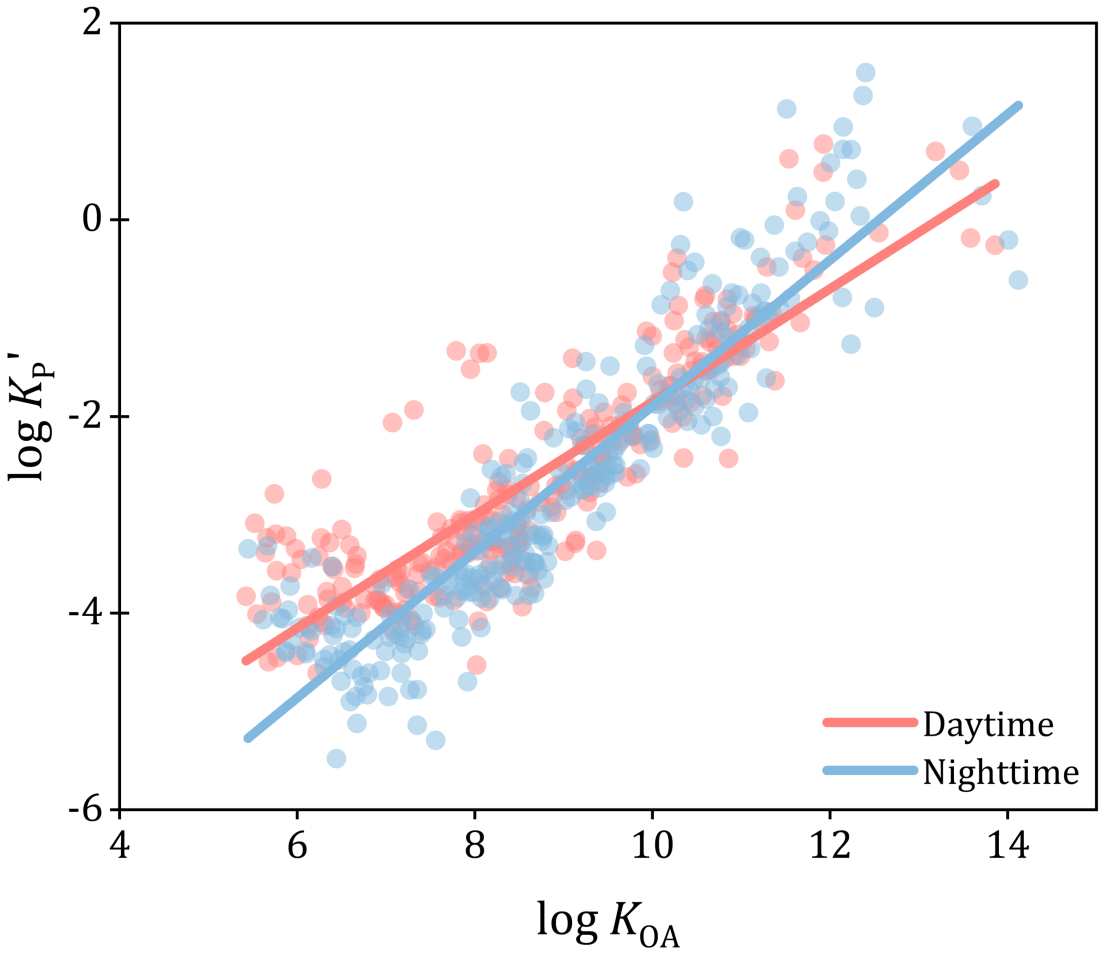

Fig. S3. Comparison the regression lines of log K_P' against log K_{OA} between daytime and nighttime for total Me-PAHs

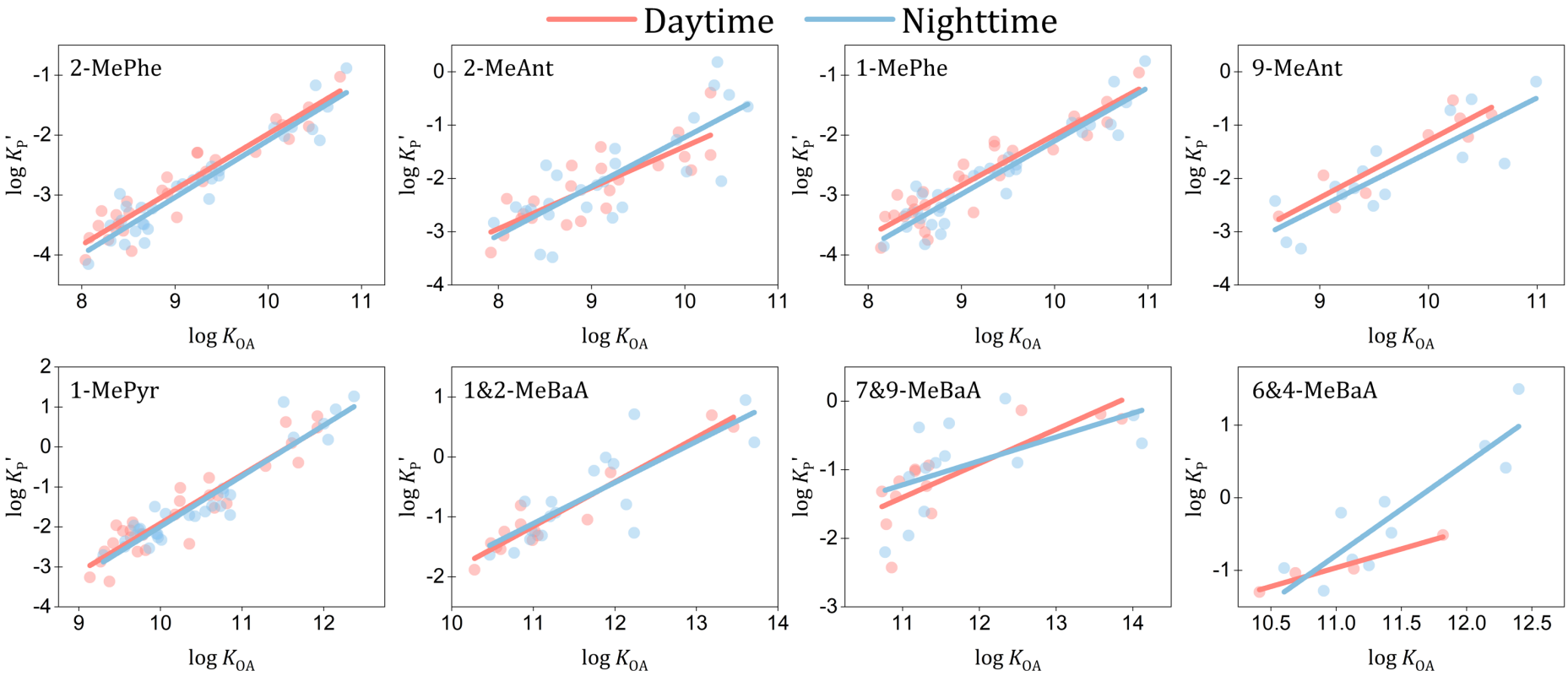

Fig. S4. Comparison of the regression lines of log K_P' against log K_{OA} between daytime and nighttime for part of individual Me-PAHs

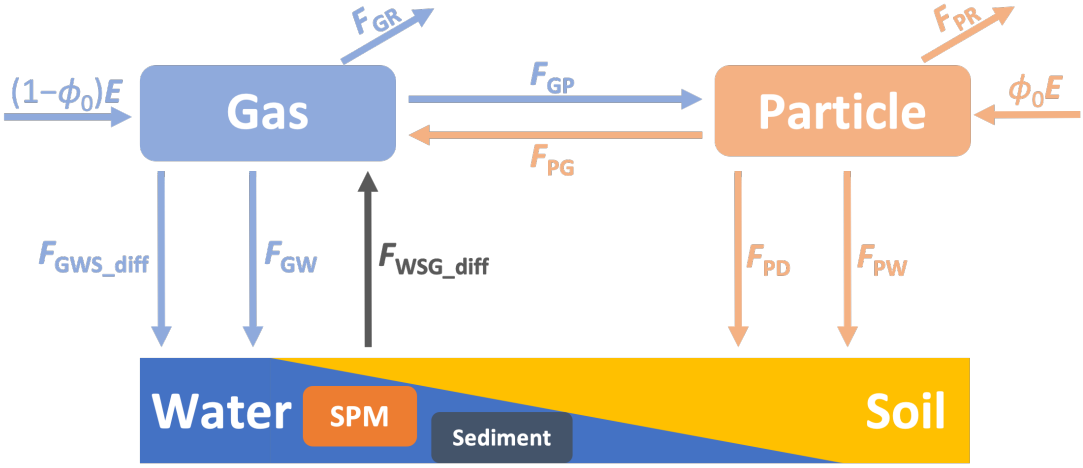

Fig. S5. The fluxes related to the gas and particle phase in the six-compartment model

(Note: F_{GR}: degradation flux of gas phase PAHs; F_{PR}: degradation flux of particle phase PAHs; F_{GP}: migration flux from gas phase to particle phase; F_{PG}: migration flux from particle phase to gas phase; F_{GWS_diff}: diffusion fluxes from gas phase to water and/or soil phases; F_{GW}: wet deposition flux of gas phase PAHs to water and/or soil phase; F_{WSG_diff}: diffusion fluxes from soil and/or water phases to gas phase; F_{PD}: dry deposition flux of particle phase PAHs to SPM and/or soil phase; F_{PW}: wet deposition flux of particle phase PAHs to SPM and/or soil phase; $(1-\phi_0)E$: emission flux of gas phase PAHs; $\phi_0 E$: emission flux of particle phase PAHs.)

The Figure was cited from our previous study:

Zhu, F. J., Hu, P. T., and Ma, W. L.: A new steady-state gas–particle partitioning model of polycyclic aromatic hydrocarbons: Implication for the influence of the particulate proportion in emissions, Atmospheric Chemistry and Physics, 23, 8583-8590, https://doi.org/10.5194/acp-23-8583-2023, 2023.